3-D LASER PULSE SHAPING FOR PHOTOINJECTOR DRIVE LASERS*

Yuelin Li[#], ANL, Argonne, IL 60439, U.S.A.
Xiangyun Chang, BNL, Upton, NY 11973, U.S.A.

Abstract

In this paper we present a three-dimensional (3-D) laser pulse shaping scheme that can be applied for generating ellipsoidal electron bunches from a photoinjector. The 3-D shaping is realized through laser phase tailoring in combination with chromatic aberration in a focusing optics. Performance of an electron beam generated from such shaped laser pulses is compared with that of a uniforma ellipsoidal, a uniform cylindrical, and a Gaussian electron beam. PARMELA simulation shows the advantage of this shaped beam in both transverse and longitudinal performances.

INTRODUCTION

The emittance of an electron beam is governed by the emittance at its birth and the growth during its propagation. If the beam is only subjected to linear force, the latter can be fully recovered with proper beam compensation. It is well known that an ellipsoidal beam with uniform charge distribution has a linear space-charge force [1-3] and hence the most expected distribution for modern high-brightness beams. Recently, several researchers looked at practical ways of generating such ellipsoidal beams, including self-evolving [4], cold electron harvesting [5], and laser pulse manipulations including spectral masking, pulse stacking, and dynamic spatial filtering [6]. In-depth analysis shows that in practical situations, the ellipsoidal beams do generate beam with lower emittance than Gaussian and cylindrical beams [1, 6-8]. Applications for such high-brightness beams include next-generation light sources such as the Linac Coherent Light Source (LCLS), high-energy colliders such as the International Linear Collider, as well as energy-recovery linacs (ERLs).

LASER PULSE SHAPING

To generate an ellipsoidal beam directly from the photocathode, the laser pulse has to be shaped in 3-D. It is well known that the longitudinal laser pulse shape can be manipulated by controlling the phase space using techniques such as DAZZLER [9] or SLIM [10]. One essence of this phase modulation is to control the phase and amplitude at certain frequencies at the same time. In the meantime, we notice that the instant frequency of a laser pulse is related to the phase by $\omega(t) = \mathrm{d}\phi(t)/\mathrm{d}t$. This gives a way of actively controlling the focal size of the laser as a function of time using the chromatic aberration of a common lens, of which the focal length can be

expressed as [11]

$$\frac{1}{f(\omega)} = [n(\omega) - 1]\left(\frac{1}{R_1} - \frac{1}{R_1}\right), \tag{1}$$

where R_1 and R_2 are the radius of curvature of the first and second surface of the lens, respectively, and n is the frequency-dependent refractive index. Clearly, the time-dependent frequency can then be mapped onto a time-dependent focal length. For an observer at the focal plane at a nominal frequency ω_0, this is equivalent to a time-dependent defocusing of the beam of

$$\delta f(t) = -\frac{f_0}{n_0 - 1}\beta\delta\omega(t), \tag{2}$$

where we assume the frequency range is small and $\beta = dn/d\omega$ is constant. For a Gaussian beam this translates into a time-dependence of the beam size at the nominal focal plane,

$$w(t) = w_0\left[1 + \left(\frac{\lambda_0\delta f(t)}{\pi w_0^2}\right)^2\right]^{1/2}. \tag{3}$$

Here, $w_0 = N\lambda_0/\pi$ is the beam waist at the nominal wavelength λ_0, and N is the numerical aperture. For $\delta f >> w_0$, we have asymptotically,

$$w(t) \cong \frac{|\delta f(t)|}{N}. \tag{3a}$$

To generate an ellipsoidal outline, the transverse beam size should be of the form:

$$w(t) = W\left[1 - \left(\frac{t}{T}\right)^2\right]^{1/2}. \tag{4}$$

Here, W is the maximum transverse beam size at $t = 0$ and $2T$ is the laser pulse duration.

From Eqs. (3-4), we have

$$|\delta\omega(t)| = \Delta\omega\left[1 - \left(\frac{t}{T}\right)^2\right]^{1/2}, \tag{5}$$

where $\Delta\omega = (n_0-1)NW/\beta f_0$ is the bandwidth of the pulse; hence the phase of the pulse is

$$\phi(t) = \int[\omega(t) - \omega_0]dt$$
$$= -\omega_0 t \pm \frac{\Delta\omega}{2}\left[t\left(1 - \left(\frac{t}{T}\right)^2\right) + T\sin^{-1}\frac{t}{T}\right]. \tag{6}$$

To make the pulse intensity constant over time, i.e., $|A(t)|^2/w(t)^2 = $ constant, the amplitude of the pulse is thus

$$A(t) = A_0\left[1 - \left(\frac{t}{T}\right)^2\right]^{1/2}. \tag{7}$$

With a transverse top-hat spatial profile, the field $E(t) = A(t)\exp[i\phi(t)]$ represents a 3-D ellipsoidal pulse at the nominal focal plane at λ_0. The time domain representation of the pulse and its spectrum are shown in Fig. 1.
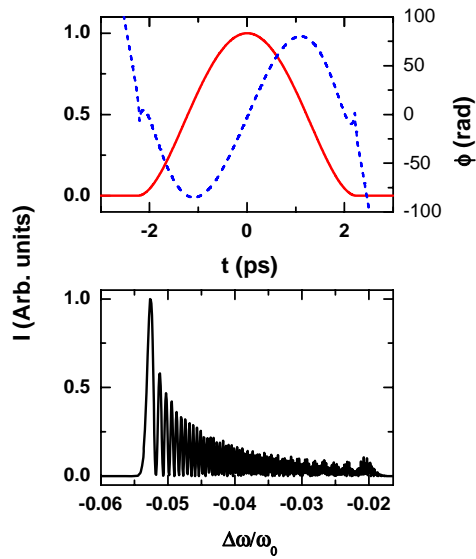
Figure 1: Laser pulse calculated using Eqs. (6) and (7). The intensity and phase in the time domain (top) and its spectrum (bottom).

Note that the above model used Gaussian beam geometrical optics, and the effects of group velocity delay (GVDE) and group velocity dispersion (GVDI) due to the varying thickness across the aperture of the lens are not included [11]. It does not take into account the wave property of the light. To evaluate the effects of GVDE and GVDI, we use the method elaborated by Kempe et al. [12] to calculate the temporal-spatial distribution of the pulse near the focus of a lens. The calculation assumes a collimated beam with top-hat intensity distribution for the input and was performed in the frequency domain. The final result was Fourier transformed into the time domain to give the laser intensity distribution at the focal plane as a function of time. Figure 2 shows one example of such a shaped pulse generate by sending a pulse in Fig. 1 though a zone plate (a zone plate has similar chromatic aberration as a lens).

Clearly, this shaped pulse differs from an ideal ellipsoid. It has substantial substructures. The deviation from an ideal ellipsoidal is not unexpected due to the group delay across the plate, which is the source for the distortion at the beginning and the end of the pulse. This has been studied theoretically and experimentally by a few authors and is an important effect in focusing short-duration, short-wavelength laser light [12].

The substructure is due to the fringes typical of the Fourier transform of a square waveform. As is shown below, those substructures seem to have minimum impact on the performance of the beam.

BEAM SIMULATION

To evaluate the performance of this shaped laser beam, preliminary simulations using PARMELA were performed and compared with other beam shapes for the following setting.

The simulation followed a setup for the design of the electron cooling ring injector for Relativistic Heavy Ion Collider [13]. The gun is a 1.5-cell rf gun at 703.75 MHz with maximum field on axis of 29.5 MV/m and maximum field on surface at 49.3 MV/m. The rf initial phase is set at 40 degrees. Beam distortion due to image charge is considered. The gun is followed with a drift space before entering a linac.

A series of simulations were performed using PARMELA. The simulations compared the performance of the 3-D laser pulse against three standard cases (see Table 1): c) a perfect ellipsoidal beam, d) a cylindrical beam, and e) a transversely uniform but longitudinally Gaussian beam. For the shaped beam, two cases were tested: a) without considering the substructures and b) with. The simulations use the parameters listed in Table 1. Both the longitudinal and the transverse emittances are compared at the exit of the gun. In total, 46,600 particles are used in each simulation, representing 0.15 nC of charge. The low charge is used due to the relatively low rf field in this setup.

The emittances as a function of the propagation distance are shown in Fig. 3. In general, the performances
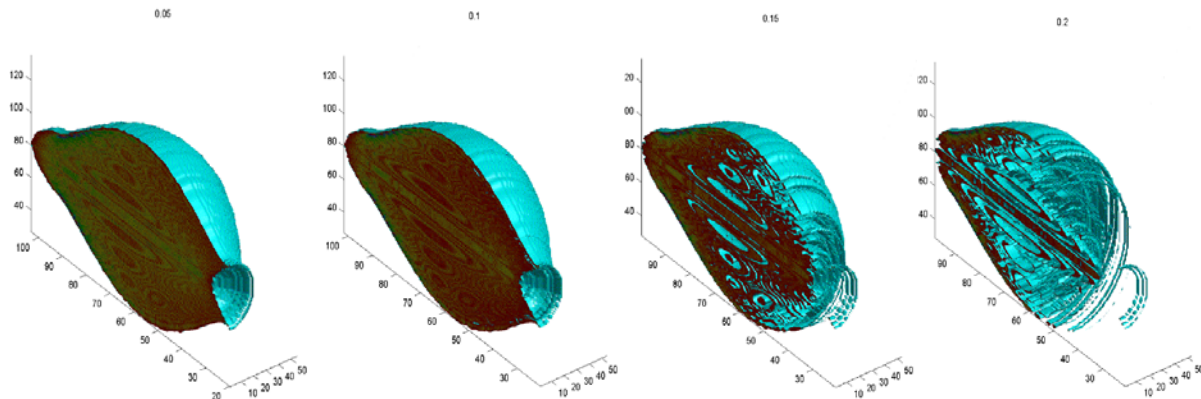

Figure 2: An ellipsoidal laser pulse. The isosurface plots show the structure at different laser intensities of 0.05, 0.1, 0.15, and 0.2. The pulse is generated using a zone plate with 20-mm diameter and 150-mm focal length at 249 nm. The pulse parameter is shown in Table 1, case b.
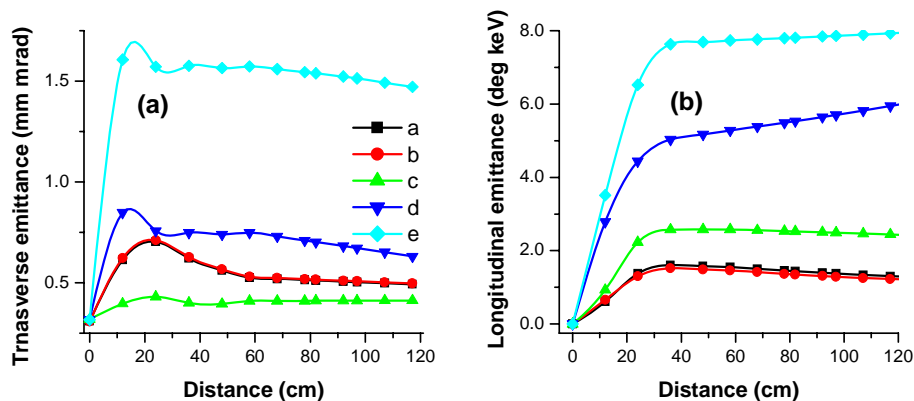
Figure 3: Transverse (a) and longitudinal (b) emittances as a function of propagation distance. The labels correspond to those in Table 1. Clearly, the shaped pulse has a better performance in comparison with those of the cylindrical and Gaussian form, even with the presence of the substructures shown in Fig. 2. The gun exit is located at 48 cm, followed a drift space.

Table 1. Initial Beam Conditions

	Length (ps)	Radius (mm)
a.Shaped, no substructure	17	1.28
b.Shaped, substructure	17	1.28
c. Ideal ellipsoid	18	1.28
d. Ideal cylinder	18	1.13
e. Ideal Gaussian	$\sigma = 3.82$, truncated at 9	1.13

of the shaped-pulse cases closely trail the performances of the ideal ellipsoidal beam in both longitudinal and transverse emittances. More remarkably, the substructure, as shown in Fig. 2, has almost no impact on the performance of the beam in this setup. It will be interesting to perform simulations with bending magnets, such as a chicane structure to evaluate the influence of coherence transition radiation, which is detrimental to cylindrical and Gaussian beams but has minimum impact on an ideal ellipsoidal beam. One simulation indicates that after accelerated to high beam energy, the ellipsoidal beam shape will be destroyed but the low emittance of the beam is preserved [8], making it favorable for application in free-electron lasers such as LCLS and ERLs.

SUMMARY

We described a scheme for generating an ellipsoidal laser pulse and performed preliminary simulations comparing the electron beam generated from this laser beam with an ideal ellipsoidal beam, a cylindrical beam, and a Gaussian beam. It is shown that although the beam generated still defers from an ideal ellipsoidal beam, it has clearly better performance than a cylindrical beam and a Gaussian beam in providing smaller transverse and longitudinal emittance.   Further beam simulations are needed to investigate the coherent synchrotron radiation effect for setup relevant to LCLS and future ERLs.

REFERENCES

[1] F. Sacherer, IEEE Trans. Nucl. Sci. NS-**18**, 1105 (1971).

[2] I.M. Kapchinskij, V.V. Vladimirskij, Conference on High Energy Accelerators and Instrumentation, CERN, Geneva, 274 (1959).

[3] P.M. Lapostolle, IEEE Trans. Nucl. Sci. NS-**18**, 1101 (1971).

[4] O.J. Luiten, S.B. van der Geer, M.J. de Loos, F.B. Kiewiet, and M.J. van der Wiel, Phys. Rev. Lett **93**, 094802 (2004).

[5] B.J. Claessens, S.B. van der Geer, G.Taban, E.J.D. Vredenbregt, and O.J. Luiten, Phys. Rev. Lett **95**, 164801 (2005).

[6] C. Limborg-Deprey and P. Bolton, Nucl. Instrum. Methods A**557**, 106 (2006).

[7] J.B. Rosenzweig et al., Nucl. Instrum. Methods A**557**, 87 (2006).

[8] S.B. van der Geer, M.J. de Loos, T. van Oudheusden, W.P.E.M. op't Root, M.J. van der Wiel, and O.J. Luiten, Phys Rev. ST-AB **9**, 044203 (2006).

[9] P. Tournois, Opt. Commun. **140**, 245 (1997).

[10] A.M. Weiner, D.E. Leaird, J.S. Patel, and J.R. Wullert, Opt. Lett. **15**, 326 (1990).

[11] M. Born and E. Wolf, *Principles of Optics*, University Press, Cambridge, UK, 2003.

[12] M. Kempe, U. Stamm, B. Wilhelmi, and W. Rudolph, J. Opt. Soc. Am. B**9**, 1158 (1992).

[13] I. Ben-Zvi et al., Nucl. Instrum. Methods A**557**, 28 (2006).